Centrin-mediated Microtubule Severing during Flagellar Excision in *Chlamydomonas reinhardtii*

M. A. Sanders and J. L. Salisbury

Laboratory for Cell Biology, Center for NeuroSciences, School of Medicine, Case Western Reserve University, Cleveland, Ohio 44106

Abstract. *Chlamydomonas* cells excise their flagella in response to a variety of experimental conditions (e.g., extremes of temperature or pH, alcohol or detergent treatment, and mechanical shear). Here, we show that flagellar excision is an active process whereby microtubules are severed at select sites within the transition zone. The transition zone is located between the flagellar axoneme and the basal body; it is characterized by a pair of central cylinders that have an H shape when viewed in longitudinal section. Both central cylinders are connected to the A tubule of each microtubule doublet of the transition zone by fibers (~5 nm diam). When viewed in cross section, these fibers are seen to form a distinctive stellate pattern characteristic of the transition zone (Manton, I. 1964. *J. R. Microsc. Soc.* 82:279–285; Ringo, D. L. 1967. *J. Cell Biol.* 33:543–571). We demonstrate that at the time of flagellar excision these fibers contract and displace the microtubule doublets of the axoneme inward. We believe that the resulting shear force and torsional load act to sever the axonemal microtubules immediately distal to the central cylinder.

Structural alterations of the transition zone during flagellar excision occur both in living cells and detergent-extracted cell models, and are dependent on the presence of calcium ($\geq 10^{-6}$ M). Immunolocalization using monoclonal antibodies against the calcium-binding protein centrin demonstrate the presence of centrin in the fiber-based stellate structure of the transition zone of wild-type cells. Examination of the flagellar autotomy mutant, *fa-1*, which fails to excise its flagella (Lewin, R., and C. Burrascano. 1983. *Experientia.* 39:1397–1398), demonstrates that the *fa-1* transition zone also contains centrin. However, *fa-1* lacks the ability to completely contract the fibers of the stellate structure. We conclude that flagellar excision in *Chlamydomonas* involves microtubule severing that is mediated by the action of calcium-sensitive contractile fibers of the transition zone. These observations have led us to question whether microtubule severing may be a more general phenomenon than previously suspected and to suggest that microtubule severing may contribute to the dynamic behavior of cytoplasmic microtubules in other cells.

MICROTUBULES are important elements of cytoplasmic structure that show dynamic behavior in interphase and mitotic cells; they comprise the major structural component of centrioles, basal bodies, and flagella (Schliwa, 1986). The study of cilia and flagella has provided much of the conceptual basis for understanding microtubule function in general (Gibbons, 1981; Satir, 1976). The green alga *Chlamydomonas reinhardtii* serves as a particularly useful model system for structural, biochemical, physiological, and genetic dissection of these motile organelles (Huang, 1986; Lefebvre and Rosenbaum, 1986; Randall et al., 1967; Ringo, 1967; Witman et al., 1972).

Chlamydomonas, like many other organisms, cast off their flagella in response to experimental treatments such as extreme pH, heat, alcohol or other noxious agents, and mechanical shear (Blum, 1971; Lewin et al., 1982; Ringo, 1967; and see Bloodgood, 1974 for flagellar loss by resorption). The excision process is known to involve calcium ions; treatments that increase Ca^{2+} levels within the flagellum have been used to induce flagellar excision in a variety of cell types (Goldstein, 1974; Huber et al., 1986; Rosenbaum and Carlson, 1969; Thompson et al., 1974; Watson et al., 1961). Electron microscopic analysis has revealed that flagellar excision occurs just distal to the transition zone, a structurally specialized region between the flagellar axoneme and the basal body (Blum, 1971; Cavalier-Smith, 1974; Manton, 1964; Randall et al., 1967; Ringo, 1967). *Chlamydomonas* and all other chlorophyll b-containing motile plant cells show unique structural features of the transition zone (Moestrup, 1982). These include a pair of central cylinders that have an H shape when viewed in longitudinal section and fibers which connect the central cylinders to the doublets of the transition zone; these fibers form a distinctive stellate pattern when viewed in cross section (see below; Cavalier-

J. L. Salisbury's present address (as of August 1, 1989) is Department of Biochemistry and Molecular Biology, Mayo Clinic, Rochester, Minnesota 55905.

Smith, 1974; Lewin et al., 1982; Manton, 1964; Randall et al., 1967; Ringo, 1967). Although flagellar excision has been recognized and studied for nearly half a century, the actual mechanism, called autotomy or "self cutting" (Lewin et al., 1982; Lewin and Burrascano, 1983), has remained elusive.

In this study, we find that flagellar excision is mediated by a calcium-sensitive alteration of transition zone structure. Our studies with monoclonal anti-centrin antibodies reveal that fibers of the transition zone stellate structure contain centrin. Centrin is a 20,000-M_r calcium-binding protein that was originally identified as a component of fiber-based, basal body-associated, contractile organelles of algal cells (Salisbury et al., 1984, 1988). cDNA clones coding for centrin (called caltractin by some workers) have recently been isolated and sequenced (Huang et al., 1987). During flagellar excision, stellate structure centrin-containing fibers of the transition zone contract and displace the microtubule doublets of the transition zone inward thus severing them.

Materials and Methods

Cell Culture

Chlamydomonas reinhardtii, wild-type strain 137c, and the flagellar autotomy mutant *fa-1* (Lewin and Burrascano, 1983) were obtained from the *Chlamydomonas* culture collection at Duke University (E. H. Harris, Durham, NC). Cultures were maintained in Sager and Granick (1954) medium I in 10-ml tubes under a 14:10-h light/dark cycle at 24°C.

Flagellar Excision in Living Cells

Cultures were harvested by centrifugation and resuspended in culture medium containing buffer A (10 mM Tris-HCl, 1 mM NaH_2PO_4, 2 mM sodium acetate, pH 7.0) to a final density of 10^6 cells/ml. Cells were subjected to pH shock by reducing the pH to 4.3 with 1.0 N acetic acid for 2 min while vigorously stirring with a magnetic bar, and then returned to neutral pH with 1.0 N KOH. Aliquots of cells were collected before (preshock condition), during shock (shock condition), and 5 min after shock (recovery condition) and processed for electron microscopy.

Flagellar Excision in Detergent Extracted Cell Models

Cells were collected by centrifugation and washed twice in buffer B (10 mM Tris-HCl, 5 mM EGTA, 3 mM $MgSO_4$, pH 7.0). Cell pellets were gently resuspended in 0.5 ml buffer B and then extracted by adding 10 vol of extraction buffer C (10 mM Tris-HCl, 5 mM EGTA, 3 mM $MgSO_4$, 0.01% Nonidet, pH 7.0). Cell models were treated in buffer C with the free calcium level adjusted with a Ca^{2+}/EGTA buffer system (Fabiato and Fabiato, 1979). Some experiments were also carried out in buffer C containing a protease inhibitor cocktail which included 2 mM PMSF, 10 μg/ml chymostatin, 400 kallikrein units aprotinin, and 0.3 mg/ml soybean trypsin inhibitor (protease inhibitors were purchased from Sigma Chemical Co., St. Louis, MO).

Electron Microscopy

Fixation was carried out according to a modification of the procedure of McDonald (1984). Cells were fixed in 3% glutaraldehyde buffered with 10 mM Hepes, pH 7.2, for 2 h at 4°C. After a buffer wash (10 mM Hepes, pH 7.2) the samples were postfixed in 1% osmium tetroxide and 0.8% $K_3Fe(CN)_6$ in 4 mM phosphate buffer, pH 7.2, for 30 min at 4°C. Samples were washed with deionized water, mordanted with 0.15% aqueous tannic acid for 1 min at room temperature, washed with deionized water, and stained with 2% aqueous uranyl acetate for 2 h in the dark. After washing with deionized water, the samples were dehydrated through an ethanol series, cleared with propylene oxide, and embedded in Poly/Bed 812. Blocks were polymerized at 60°C for 48 h. Silver sections were collected on copper grids, poststained at room temperature with aqueous 2% uranyl acetate for 15 min, followed by Reynold's lead citrate for 15 min. Sections were observed and photographed on a JEOL 1200 EX electron microscope.

Immunofluorescence

Cells were fixed in 4% fresh paraformaldehyde buffered with 10 mM Hepes, pH 7.0, for 15 min and allowed to adhere to eight-well glass slides (Carlson Scientific, Peotone, IL), which had been pretreated with 0.1% polyethylenimine (Sigma Chemical Co.). After three washes in 10 mM Hepes buffer the cells were simultaneously permeabilized and blocked for nonspecific binding by treating the slides with 5% goat serum (Gibco Laboratories, Grand Island, NY), 5% glycerol, and 5% DMSO for 30 min at 37°C. The cells were incubated in primary anti-centrin monoclonal antibody (17E10; Salisbury et al., 1988, diluted 1:100 in the blocking and permeabilization buffer) for 3 h, washed three times in PBS, and reacted with secondary fluorescein-conjugated goat anti-mouse IgG (Organon Teknica-Cappel, Malvern, PA, diluted 1:400 in the blocking and permeabilization buffer) for 1 h. The preparations were washed for 15 min in three changes of PBS, mounted in 50% glycerol/50% PBS, pH 8.5, containing 2% *N*-propylgallate (Eastman Kodak Co., Rochester, NY), and observed using a Nikon Optiphot microscope equipped for epifluorescence (excitation 450–490 nm, barrier filter 590 nm). Immunofluorescence images were recorded on Hypertech film (Microfluor Ltd., Stony Brook, NY) with 10–20-s exposures, and developed in D-19 developer at 68°F for 4 min.

Immunogold Labeling

Chlamydomonas 137c and *fa-1* cells were fixed in 1% glutaraldehyde buffered with 10 mM Hepes, pH 7.2, for 15 min at 4°C and washed 3 times in 10 mM Hepes buffer. Free aldehyde groups were reduced by treatment with aqueous sodium borohydride (7 mg/ml) for 15 min at 4°C and washed three times with 10 mM Hepes. Samples were dehydrated through an ethanol series at −20°C. Samples were infiltrated with Lowicryl resin (Pella, Inc., Redding, PA), cured at −20°C using UV light, sectioned, and collected on formvar-coated nickel grids. Sections were hydrated with deionized water for 10 min, blocked in 0.1% BSA and 5% normal goat serum in Tris-buffered saline (TBS; 10 mM Tris HCl, 150 mM NaCl, pH 7.4) for 1 h, incubated in primary monoclonal antibody (17E10, diluted 1:100 in TBS, pH 7.4, containing 0.1% BSA and 5% normal goat serum) for 2 h, washed for 15 min with several changes of TBS, and reacted with secondary goat anti-mouse IgG conjugated to 10 nm colloidal gold (Janssen Life Science Products, Piscataway, NJ; 1:40 dilution in TBS, pH 8.2, containing 0.1% BSA and 5% normal goat serum) for 1 h. Sections were washed as above, postfixed in aqueous 1% glutaraldehyde, washed with deionized water, and poststained as above before observation.

Results

Chlamydomonas Flagellar Excision

Vegetative *Chlamydomonas* cells normally have a pair of apically inserted flagella, each ~11 μm in length. The flagellar membrane represents ~10% of the total surface area of the cell (Lewin et al., 1982); for wild-type *Chlamydomonas* cells this represents the only "naked" membrane exposed to the environment as the remainder of the cell is covered by a cell wall. Cells respond to a variety of environmental stress situations by casting off their flagella by a process known as excision or autotomy ("self cutting"; Blum, 1971; Lewin and Burrascano, 1983); this effectively eliminates the naked membrane surface exposed to environmental trauma. Fig. 1 illustrates *Chlamydomonas* cells in midlongitudinal section before and immediately after pH shock-induced flagellar excision. Both flagella excise distal to the transition zone leaving the basal bodies and associated structures intact within the cell body. Note that the plasma membrane has resealed over the basal bodies, the distance between the flagellar apparatus and the nucleus has shortened, and that nuclear shape has been altered; nuclear movement and shape changes are due to contraction of the centrin-based nucleus–basal body connector as reported earlier (Salisbury et al., 1987; Wright et al., 1985).

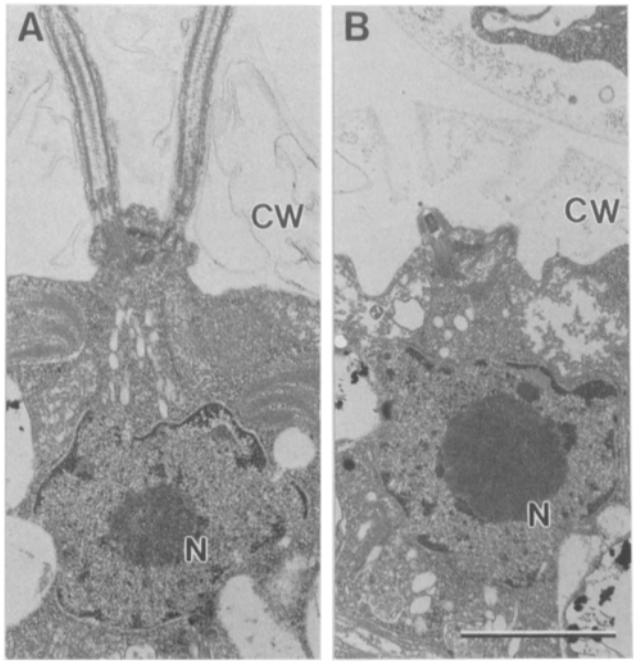

Figure 1. Electron micrographs of medial longitudinal sections of *Chlamydomonas reinhardtii* cells before (*A*) and immediately after (*B*) pH shock-induced flagellar excision. Note that flagella excise just distal to the transition zone and that the plasma membrane rapidly seals over the site of flagellar excision. Also, the distance between the flagellar apparatus and the nucleus has decreased and the nucleus has undergone a subtle shape change. CW, cell wall; *N*, nucleus. Bar, 2 μm.

Alterations in Transition Zone Structure

Fig. 2, *A–D* illustrates normal basal body, transition zone, and axoneme structure. The flagellar axoneme is ~0.2 μm in diameter and is composed of nine outer doublet microtubules arranged circumferentially around a central pair of microtubules (Fig. 2, *A* and *B*). Each doublet consists of a complete microtubule, the A tubule, consisting of 13 protofilaments, and a partial microtubule, the B tubule, consisting of 11 protofilaments (Tilney et al., 1973). The cross section in Fig. 2 *B* shows nexin links between adjacent outer doublet microtubules just proximal to the region where dynein arms occur along the axoneme. The axoneme is anchored in the cell at the basal body. The basal body consists of a cylindrical set of nine microtubule triplets (0.5–0.75 μm long) and is further characterized by the absence of dynein, nexin, and spoke proteins (Fig. 2, *A* and *D*). Each triplet consists of an A and B tubule which are continuous with the axonemal microtubules, and an additional partial microtubule, the C tubule. The transition zone connects the axoneme to the basal body and is characterized by microtubule doublets and a pair of central cylinders that have an H shape when viewed in longitudinal section (Fig. 2 *A*). The distal cylinder is 80 nm in diameter, 100–120 nm long, and closed at its proximal end. The proximal cylinder is also 80 nm in diameter, 50–70 nm long, and open at both ends. The H piece cylinders are connected to the A tubules of the microtubule doublets by fibers (~5 nm diam) which form a distinctive stellate pattern when viewed in cross section (Fig. 2 *C*). The organization of these fibers is complex, however, careful analysis reveals that they connect every other A tubule and are arranged in a spiral for six to seven turns along the length of the H piece (and see Manton, 1964).

Fig. 2, *E–L* illustrates transition zone structure during flagellar excision and subsequent regrowth. At the time of flagellar excision, the transition zone undergoes dramatic structural alterations. The fibers of the stellate structure contract around the outer wall of the central cylinder in the distal 1/3 of the H piece (Fig. 2, *E* and *G*, Fig. 3, *B–E*). This displaces the doublet microtubules inward and results in a 12% reduction in the overall diameter of the transition zone, a 42% reduction of the distance between each A tubule and the H piece cylinder, and a change in pitch or doublet angle relative to the radius of the transition zone from 9.6° to 22.1° (compare Fig. 2, *C* with *G*, Fig. 3, *A* with *B–E*, and see Table I). The diameter of the basal body and arrangement of microtubule triplets are not significantly affected during excision. Concomitant with flagellar excision, the plasma membrane seals over the transition zone (Fig. 2 *E*). By 5 min after exci-

Table I. Characteristics of Transition Zone Structure before and after pH Shock-induced Flagellar Excision

Condition	Transition zone diameter	Tubule distance to central cylinder	Doublet angle*
	nm	*nm*	
Wild-type cells			
(*A*) Preexcision	186 ± 9.68	31.2 ± 1.7	9.6° ± 5.7°
(*B*) Postexcision	164 ± 7.84	18.2 ± 2.8	22.1° ± 6.5°
(*C*) 5 min postexcision	194 ± 7.13	32.1 ± 2.8	8.9° ± 4.9°
(*D*) Difference between A and B	22 (12%)	13.0 (42%)	12.5°
Flagellar autotomy mutant *fa-1*			
(*E*) Preshock	183 ± 6.4	31.4 ± 3.8	10.2° ± 3.9°
(*F*) Postshock	185 ± 6.6	29.8 ± 3.7	11.8° ± 4.1°
(*G*) Difference between E and F	3 (1%)	1.6 (5%)	1.6°

* The doublet angle (pitch) is determined from cross sections at the distal 1/3 of the transition zone; it is the complement of the acute angle formed by a line bisecting the A and B tubule and a radius passing through the center of the A tubule and the center of the H piece. Values represent the mean of determinations from six transition zones ± their standard deviations.

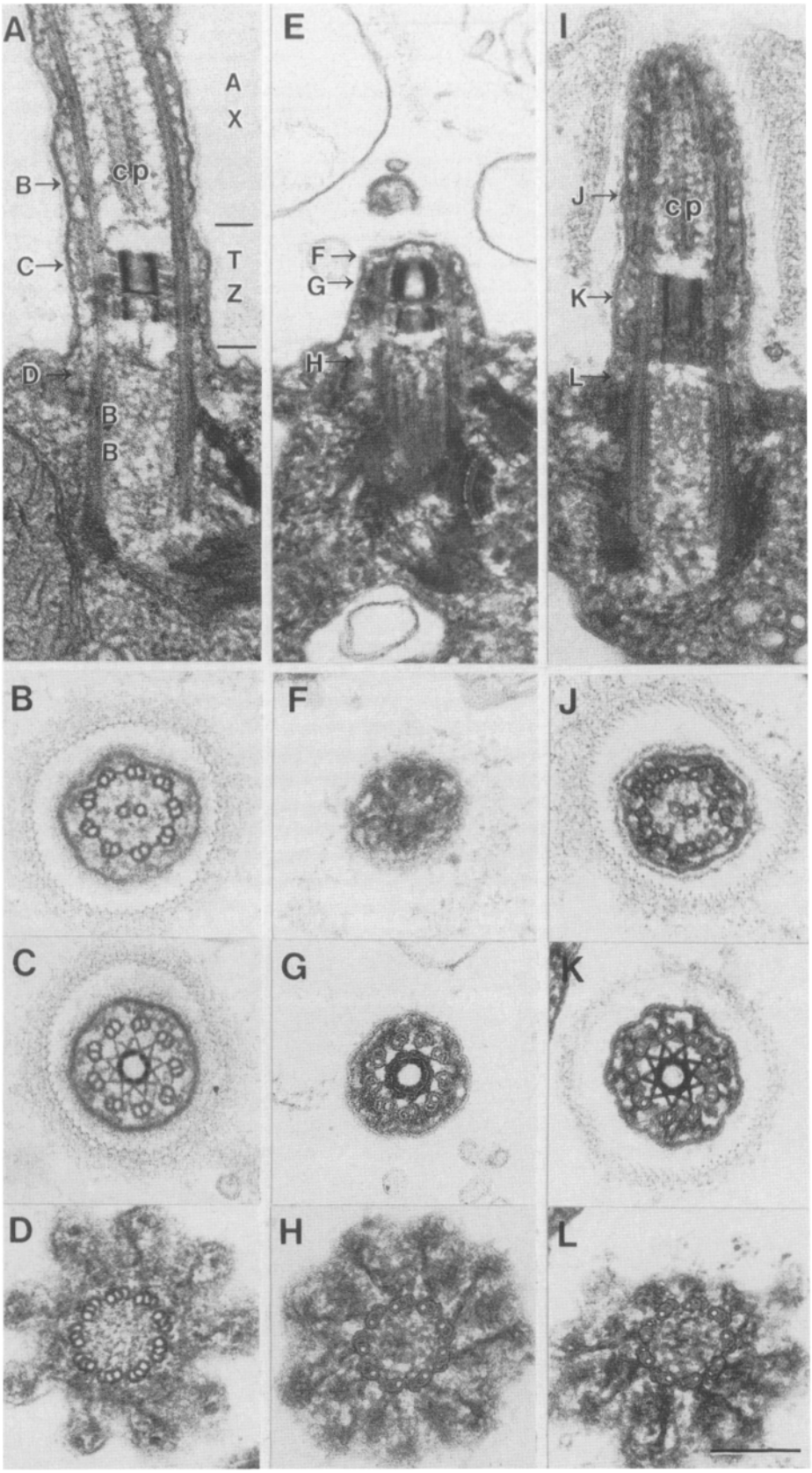

Figure 2. Electron micrographs of the flagellar transition region in *Chlamydomonas reinhardtii* before (*A–D*), immediately following (*E–H*), and after 5 min recovery (*I–L*) from pH shock–induced flagellar excision. (*A*) Longitudinal section of the axoneme (*AX*)/basal body (*BB*) region illustrating the transition zone (*TZ*) H piece and fibers of the stellate structure. Arrows labeled *B–D* indicate the approximate level of cross section for *B–D*. (*B*) Cross section of the axoneme distal to the transition zone illustrating the 9 + 2 pattern of the axoneme microtubules and nexin links connecting adjacent doublets. (*C*) Cross section of the transition zone illustrating the stellate pattern of fibers that connect the A tubule of each doublet to the central cylinder of the H piece. This is the active zone of contraction during flagellar excision (compare with *G*). (*D*) Cross section of a basal body illustrating the nine triplets of microtubules and the surrounding fibers which anchor the basal body to the plasma membrane. (*E*) Longitudinal section of a transition zone and basal body immediately after flagellar excision. Note that the distal region of the transition zone is constricted, the H piece distal cylinder wall appears thicker, and the plasma membrane has resealed over the transition zone. Arrows labeled *F–H* indicate the approximate level of cross section for *F–H*. (*F*) Cross section of the distal-most region of the transition zone. (*G*) Cross section of the transition zone illustrating contraction of the stellate fibers around the central cylinder and displacement of the microtubule doublets toward the H piece cylinder (compare with *C*). (*H*) Cross section of the basal body; note that its diameter and the orientation of microtubule triplets have not changed significantly. (*I*) Longitudinal section of a newly forming axoneme, the transition zone, and basal body after 5 min recovery from flagellar excision; note that the axoneme has grown to ~0.5 μm in length. Arrows labeled *J–L* indicate the approximate level of cross section for *J–L*. (*J*) Cross section of the growing axoneme distal to the transition zone. (*K*) Cross section of the transition zone illustrating the return to the preexcision stellate pattern (compare with *C* and *G*). (*L*) Cross section of the basal body. *B–D*, *F–H*, and *J–L* are from nonconsective serial sections. Bar, 0.2 μm.

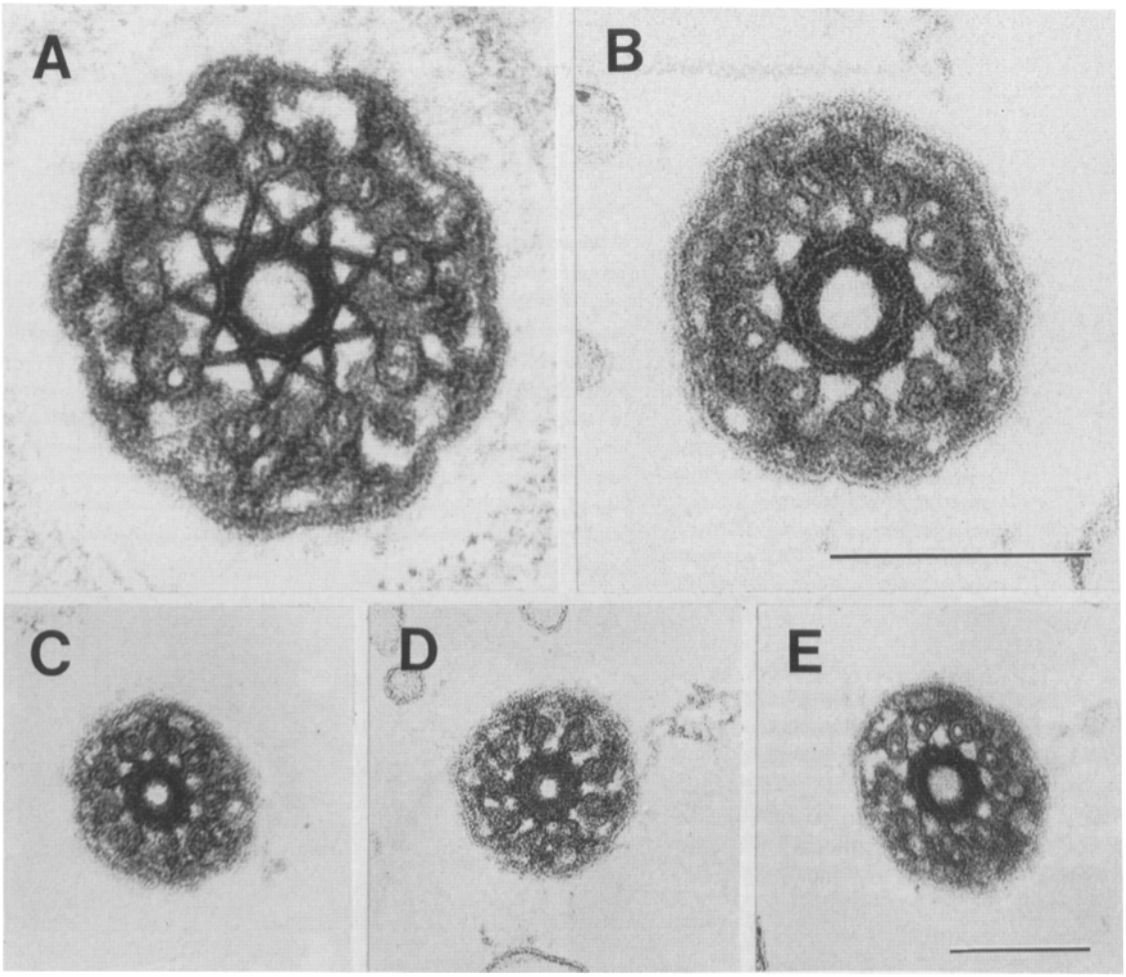

Figure 3. Cross sections of the distal 1/3 region of the transition zone. The essential features of transition zone structure in the (*A*) stellate, and (*B*) contracted configurations are illustrated at high magnification. Further examples of the contracted configuration are shown in *C–E*. Bar, 0.2 μm.

sion the contracted fibers of the transition zone have returned to the stellate configuration (Fig. 2 *K*) and the flagellar axoneme has begun to regrow (Fig. 2 *I*). In Fig. 3, *A* and *B* illustrate the essential features of transition zone structure in the stellate and contracted configurations at higher magnification. Examples of three additional contracted transition zone stellate structures are shown in Fig. 3, *C–E*.

Flagellar Excision Requires Calcium

Flagellar excision and the structural alterations in the transition zone described above are sensitive to the prevailing levels of free calcium in the medium. Living cells fail to excise their flagella after pH shock if the free calcium level in the medium is buffered at or below 10^{-7} M. Magnesium will not substitute for calcium. We have also observed that under conditions where living cells are blocked in flagellar excision by the absence of Ca^{2+}, they quickly die in response to pH shock. In detergent-extracted cell models, where the flagellar membrane has been removed, calcium shock (Ca^{+2} levels raised to $\geq 10^{-6}$ M) alone is sufficient to induce flagellar excision (Fig. 4). When the Ca^{+2} level is held at or below 10^{-7} M, neither flagellar excision nor the structural alterations in the transition zone occur. Electron microscopy of detergent-extracted cell models after calcium shock shows that the stellate structure contracts and flagella are excised in a manner similar to intact cells (not shown).

Centrin Localization in the Transition Zone

Fig. 5 illustrates indirect immunofluorescence using monoclonal anti-centrin antibodies and reveals the centrin-based cytoskeleton of *Chlamydomonas* as described earlier (Salis-

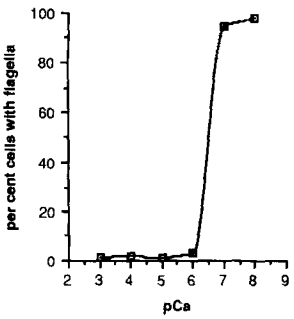

Figure 4. Flagellar excision requires calcium. NP-40–extracted cell models were treated with Ca^{2+} levels indicated on the abscissa and then scored for flagellar excision. Note that flagellar excision occurs between pCa 6 and 7.

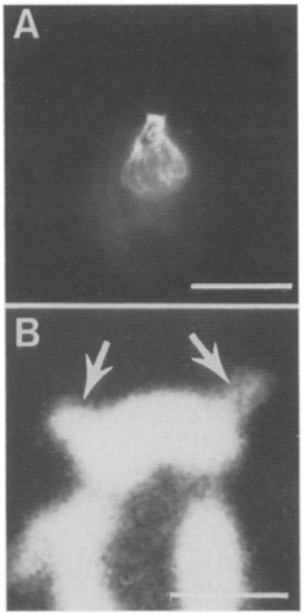

Figure 5. Indirect immunofluorescence staining of centrin using monoclonal anti-centrin 17E10 and fluorescein-conjugated secondary antibodies in *Chlamydomonas* reveals localization to the distal fiber, the nucleus-basal body connector (Salisbury et al., 1988; Wright et al., 1985), and the transition zone region of the basal bodies. (*A*) Low magnification image of whole cell centrin distribution, (*B*) High magnification image showing localization of centrin in the transition zone (*arrows*). Bars: (*A*) 5 μm; (*B*) 1 μm.

bury et al., 1987, 1988). The distal fiber linking the two basal bodies, and the "nucleus-basal body connector" (Salisbury et al., 1988; Wright et al., 1985), stain intensely with anti-centrin antibodies. Close inspection of the fluorescence pattern also shows staining of the basal bodies in the region of the transition zone (Fig. 5 *B*). Ultrastructural investigations using monoclonal anti-centrin and colloidal gold-conjugated secondary antibodies reveal the distinct localization of centrin in the transition zone (Fig. 6). Centrin localization is particularly concentrated in the region corresponding to the fibers of the stellate structure (Fig. 6 *B*). Thus centrin occurs in the distal fiber, the nucleus-basal body connector, and also within the transition zone.

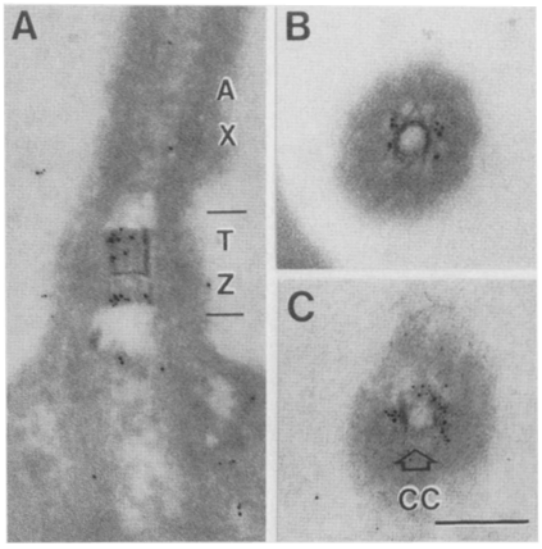

Figure 6. Centrin localization in the transition zone of wild-type cells at ultrastructural resolution using monoclonal anti-centrin 17E10 and colloidal gold-conjugated secondary antibodies. (*A*) Longitudinal section showing labeling of the transition zone H piece. (*B*) Cross section of the transition zone illustrating labeling of the stellate structure fibers. (*C*) Oblique section of the transition zone illustrating labeling of the region surrounding the central cylinder (*cc*). Quantitative analysis of gold particle density shows background levels of 9.1 and 7.5 particles/μm^2 over the resin and chloroplast, respectively, and specific labeling of 55.3 particles/μm^2 over the transition zone of wild-type cells. Bar, 0.2 μm.

fa-1: A Mutant Defective in Flagellar Excision

We have investigated transition zone structure of the flagellar excision mutant *fa-1*, which was isolated by Lewin and Burrascano (1983). *fa-1* cells fail to excise their flagella under experimental conditions that normally result in excision in wild-type cells. However, flagella can be "broken" off of *fa-1* cells by excessive mechanical shear. The flagella typically rupture at sites distal to the transition zone and the cells subsequently die (Sanders, M. A., and J. L. Salisbury, data not shown). The transition zone of *fa-1* is subtly different from wild-type cells in that the central pair of axonemal microtubules extend into the distal-most H piece cylinder beyond the point of normal termination seen in wild-type cells (Fig. 7, *A* and *C*).

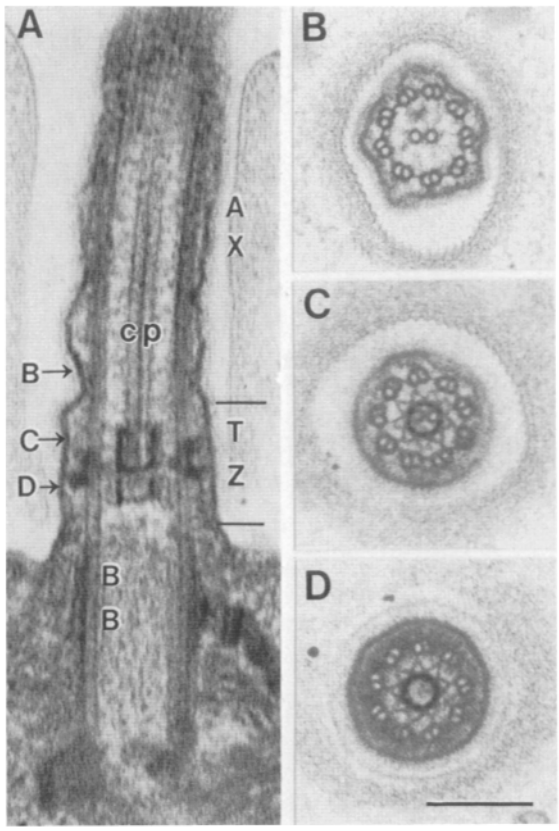

Figure 7. Electron micrographs of the transition zone of the flagellar excision mutant *fa-1*. (*A*) Longitudinal section of the axoneme (*AX*)/basal body (*BB*) region; note that the central pair (*cp*) microtubules extend into the distal cylinder of the H piece. Arrows labeled *B–D* indicate the approximate level of cross section for sections *B–D*. (*B*) Cross section of the axoneme distal to the transition zone. (*C*) Cross section of the transition zone illustrating penetration of the central pair microtubules into the distal cylinder and the otherwise normal stellate pattern of fibers that connect the A tubule of each doublet to the central cylinder of the H piece. (*D*) Cross section of the region of the proximal cylinder of the transition zone. Bar, 0.2 μm.

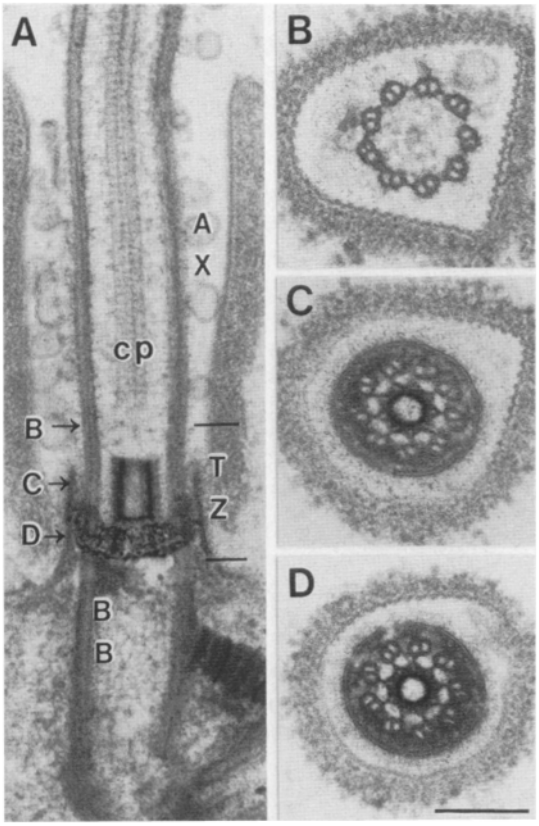

Figure 8. Electron micrographs of the transition zone of the flagellar excision mutant *fa-1* that was fixed after detergent extraction in solutions containing high free calcium (10^{-4} M). (*A*) Longitudinal section of the axoneme (*AX*)/basal body (*BB*) region; note that the central pair (*cp*) microtubules have retracted or shortened and no longer extend into the distal cylinder of the H piece. Arrows labeled *B–D* indicate the approximate level of cross section for sections *B–D*. (*B*) Cross section of the axoneme distal to the transition zone. (*C*) Cross section of the transition zone illustrating absence of the central pair microtubules in the distal cylinder. Note the failure of the stellate structure to completely contract (see Table I). (*D*) Cross section of the region of the proximal cylinder of the transition zone. Bar, 0.2 μm.

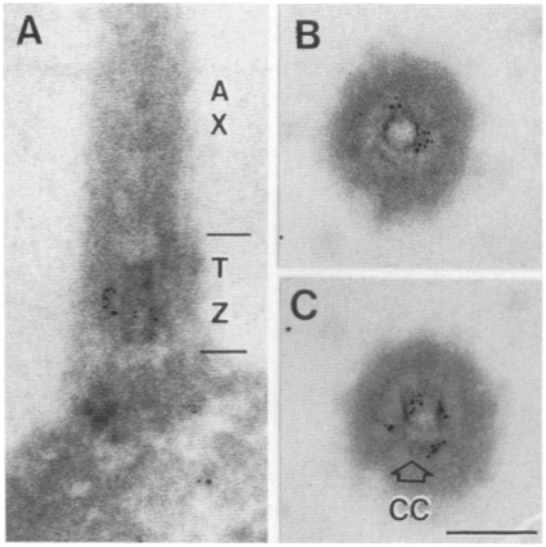

Figure 9. Centrin localization in the transition zone of *fa-1* cells at ultrastructural resolution using monoclonal anti-centrin 17E10 antibodies and colloidal gold-conjugated secondary antibodies. (*A*) Longitudinal section illustrating labeling of the transition zone H piece. (*B*) Cross section of the transition zone illustrating labeling of the stellate structure. (*C*) Oblique section of the transition zone illustrating labeling of the region surrounding the central cylinder (*cc*). Quantitative analysis of gold particle density shows background levels of 2.8 and 1.25 particles/μm^2 over the resin and chloroplast, respectively, and specific labeling of 20.5 particles/μm^2 over the transition zone of *fa-1* cells. Bar, 0.2 μm.

Detergent-extracted cell models of *fa-1* fail to excise their flagella in response to calcium treatment. After detergent extraction and calcium treatment of *fa-1* cells the central pair of microtubules no longer extend into the H piece (Fig. 8). They have either shorten or are extruded from the H piece. In addition, newly formed dense material is seen in the transition zone at the level of the proximal central cylinder of *fa-1* (Fig. 8 *A*) and wild-type (not shown) cells. Note, the flagellar membrane has been, in large part, solubilized by detergent treatment; the only remaining flagellar membrane appears surrounding the transition zone itself. These observations indicate that the *fa-1* defect is neither related to the termination point of central pair microtubules, nor simply associated with membrane permeability properties.

After calcium treatment of detergent-extracted cell models of *fa-1*, the stellate structure fails to undergo the extreme contraction seen in wild-type cell models; axoneme diameter and orientation of the outer microtubule doublets are not significantly altered (Fig. 8, *A* and *C*; Table I). Immunolocalization of centrin in *fa-1* cells appears essentially similar to that seen in wild-type cells; the distal fiber, nucleus–basal body connector (not shown), and the transition zone (Fig. 9) label with monoclonal anti-centrin and colloidal gold-conjugated secondary antibodies. Despite the apparent normal localization of centrin in these cells, we have not detected contraction of *fa-1* centrin-containing fiber systems or nuclear movement under conditions that typically result in centrin contraction in wild-type cells (Sanders, M. A., and J. L. Salisbury, unpublished observations). The basis for this defect is not yet understood. Nonetheless, the failure of *fa-1* cells to excise their flagella is related to the inability of the stellate structure to contract its fibers.

Discussion

Stellate Fiber Contraction Mediates Microtubule Severing

In this study we demonstrate that flagellar excision in *Chlamydomonas reinhardtii* is coincident with structural alterations in the transition zone. Although we cannot formally exclude the possible role of local proteolysis in the excision process, as suggested by Lewin and Lee (1985), we believe that this is unlikely because (*a*) the site of excision is precisely defined, (*b*) the excised axoneme and the transition zone do not undergo further apparent degradation, (*c*) excision occurs normally in detergent-extracted cell models in the presence of proteolytic inhibitors, and (*d*) excision is ex-

tremely rapid. Based on our structural analysis, we believe that flagellar excision occurs by a physical mechanism that may be adequately described in terms of the following fairly simple model. The transition zone fibers of the stellate structure tether the outer doublet microtubules of the axoneme to the central cylinders. The fibers of the stellate structure have elastic or contractile properties that can result in a shortening of the distance between the outer doublet tubules and the central cylinder; this shortening is sensitive to the prevailing levels of free calcium. On contraction of the stellate structure fibers, the outer doublet microtubules are drawn inward with a concomitant increase in pitch (see Table I). Thus, the doublet microtubules are subjected to an inward directed force that imposes internal stresses that ultimately result in the rupture of the microtubules.

Several alternative mechanisms for microtubule rupture are illustrated in Fig. 10. Each of these mechanisms involves a force, directed away from and either perpendicular or tangential to the wall of the microtubule. Such a force may dislodge individual tubulin subunits from the microtubule wall, thereby disrupting the tubulin lattice and destabilizing the microtubule. Alternatively, a torsional load (torque) or physical shear may rupture the microtubules when a critical stress value is exceeded. Finally, axial compression and/or tension may contribute to microtubule severing. This may be particularly true if the flagella are still beating or if other mechanical disturbances are acting on the system. Application of loads to force-bearing elements generally results in rupture through a combination of these types of mechanisms (Byars and Snyder, 1969). From our structural analysis (Fig. 2, Table I), we believe that a combination of torsional and transverse shear are likely to be the most significant factors influencing flagellar excision, especially since immotile *Chlamydomonas* mutants such as *pf-18* and detergent extracted models of wild-type cells show normal flagellar excision.

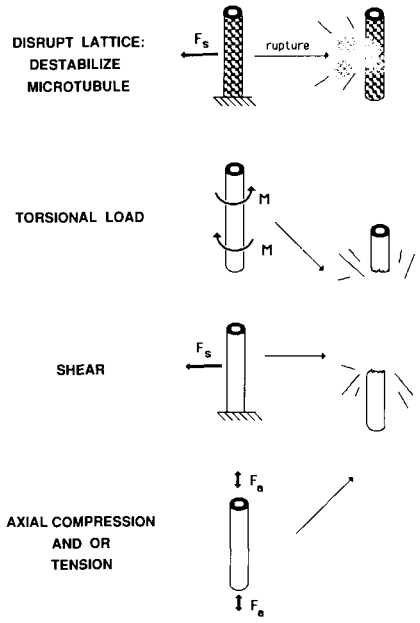

Figure 10. Diagram illustrating possible mechanisms for microtubule severing. The first case illustrates displacement of tubulin subunits from the wall of the microtubule, resulting in destabilization of the tubulin lattice and consequent microtubule rupture. The second and third cases illustrate torsional and shearing forces which may act to rupture the microtubule when some critical stress value is exceeded. Finally, rectilinear forces of axial compression and/or tension may contribute to microtubule severing.

Flagellar Excision: A New Role for the Calcium-binding Protein Centrin

Our results confirm that flagellar excision is a calcium-dependent process (Goldstein, 1974; Huber et al., 1986; Rosenbaum and Carlson, 1969; Thompson et al., 1974; Watson et al., 1961). In living *Chlamydomonas* cells, flagellar excision in response to environmental trauma requires free calcium levels to be $\geq 10^{-6}$ M. In detergent extracted cell models calcium alone ($\geq 10^{-6}$ M) is sufficient to induce flagellar excision.

Other workers have determined that the membrane surrounding the axoneme is specialized at the transition zone (see Dentler, 1981). This region of membrane is resistant to detergent extraction (Fig. 8; and see Goodenough, 1983). In addition, there are electron-dense, amorphous, connections between the membrane and the outer doublet microtubules of the axoneme (see Fig. 3). Freeze-fracture electron microscopy reveals specializations of the membrane in this region; it is characterized by intramembrane particles arranged in the form of a flagellar necklace at the transition zone, and a flagellar bracelet at the region at which the plasma membrane everts to form the flagellar membrane (Dentler, 1981; Gilula and Satir, 1972; Melkonian and Robenek, 1980; Weiss et al., 1977). Intramembrane particles of the flagellar necklace are thought to be sites of ion channels or pumps, which regulate the ionic milieu of the flagellum (Fisher et al., 1976; Gilula and Satir, 1972; Melkonian and Robenek, 1980; see also Tamm, 1988).

Our studies demonstrate that the calcium-binding protein centrin (Salisbury et al., 1984, 1988) is a component of the transition zone stellate structure. We demonstrate that the stellate structure undergoes contraction during flagellar excision and this is also dependent on calcium. Earlier studies on centrin-based cytoskeletal systems have shown that centrin is involved in basal body reorientation, nuclear movement and shape change, and also dynamic behavior during mitosis (Salisbury et al., 1984, 1987, 1988; McFadden et al., 1987; Wright et al., 1985). Common features of centrin-related motility phenomena include (*a*) calcium-sensitive contractile or elastic behavior of 3–5-nm filaments and (*b*) an association with basal bodies, centrioles, and the centrosome of all eucaryotic cells studied to date. The process of flagellar excision shares these features. This study demonstrates an additional role for centrin in mediating calcium-sensitive structural alterations of the basal body transition zone.

Does Microtubule Severing Affect Microtubule Dynamics in Other Cell Types?

In this study, we demonstrate the local severing of microtubules. To our knowledge, this is the first demonstration of microtubule severing by a physiologically relevant process in situ. From our analysis, it is apparent that the fibers of the stellate structure are calcium-sensitive force generating elements, which are active in microtubule severing and thereby

mediate flagellar excision in *Chlamydomonas*. The process of microtubule severing described here has interesting analogies with actin filament severing observed in other systems (Stossel et al., 1985). Actin severing proteins such as gelsolin, fragmin, severin, and villin mediate calcium-sensitive severing of actin filaments in amoeboid cells and in intestinal epithelial brush borders (Bretscher and Weber, 1980; Brown et al., 1982; Hasegawa et al., 1980; Stendahl and Stossel, 1980). The action of actin severing proteins results in either gel/sol transformation of the cytoplasm and/or actin filament depolymerization. Recent studies on microtubule dynamics in vitro (Keates and Hallett, 1988) and in vivo (Vigers et al., 1988) have shown that physical- or laser-induced microtubule severing can affect microtubule stability in a manner consistent with the dynamic instability model of Mitchison and Kirschner (1984*a*,*b*; see however Tao et al., 1988).

Our demonstration of microtubule severing during flagellar excision in *Chlamydomonas* has led us to question whether severing of microtubules may be a more widespread phenomenon, particularly in the centrosome region of the cell. This possibility is especially intriguing since a number of recent studies have shown that centrin or its antigenically related homologues are present in the centrosome region of all eucaryotic cells examined to date, including mammalian cells (Baron and Salisbury, 1988; Salisbury et al., 1986; Schulze et al., 1987). It is possible that microtubule severing precedes the massive reorganization of cytoplasmic microtubules in cells undergoing directed cell migration (Kupfer et al., 1982). Likewise the large scale reorganization of the microtubule complex at the interphase/mitotic transition may involve the active rupture of specific groups of microtubules.

We thank Andre Baron, Donald Coling, and Drs. R. A. Bloodgood, U. W. Goodenough, and R. A. Lewin for their helpful comments on earlier versions of the manuscript.

This work was supported by a grant from the National Institutes of Health (GM 35258) to J. L. Salisbury.

Received for publication 22 November 1988 and in revised form 17 January 1989.

References

Baron, A. T., and J. L. Salisbury. 1988. Identification and localization of a novel, cytoskeletal, centrosome-associated protein in PtK2 cells. *J. Cell Biol.* 107:2669–2678.

Byars, E. F., and R. D. Snyder. 1969. Engineering Mechanics of Deformable Bodies. 2nd ed. International Textbook Co., Scranton, PA.

Bloodgood, R. A. 1974. Resorption of organelles containing microtubules. *Cytobios.* 9:143–161.

Blum, J. J. 1971. Existence of a breaking point in cilia and flagella. *J. Theor. Biol.* 33:257–263.

Bretscher, A., and K. Weber. 1980. Villin is a major protein of microvillus cytoskeleton which binds both G and F actin in a calcium-dependent manner. *Cell.* 20:839–847.

Brown, S. S., K. Yamamoto, and J. A. Spudich. 1982. A 40,000 protein from *Dictyostelium discoideum* affects assembly properties of actin in a Ca^{2+} dependent manner. *J. Cell Biol.* 93:205–210.

Cavalier-Smith, T. 1974. Basal body and flagellar development during vegetative cell cycle and the sexual cycle of *Chlamydomonas reinhardtii*. *J. Cell Sci.* 16:529–556.

Dentler, W. L. 1981. Microtubule-membrane interactions in cilia and flagella. *Int. Rev. Cytol.* 72:1–47.

Fabiato, A., and F. Fabiato. 1979. Calculator programs for computing the composition of the solutions containing multiple metals and ligands used for experiments in skinned muscle cells. *J. Physiol. (Paris).* 75:463–505.

Fisher, G., E. S. Kaneshiro, and P. D. Peters. 1976. Divalent cation affinity sites in *Paramecium aurellia*. *J. Cell Biol.* 69:429–442.

Gibbons, I. R. 1981. Cilia and flagella of eukaryotes. *J. Cell Biol.* 91(suppl.): 107s–124s.

Gilula, N. B., and P. Satir. 1972. The ciliary necklace: a membrane specialization. *J. Cell Biol.* 53:494–509.

Goldstein, S. F. 1974. Isolated reactivated and laser-irradiated cilia and flagella. *In* Cilia and Flagella. M. A. Sleigh, editor. Academic Press, Inc., New York. 111–130.

Goodenough, U. W. 1983. Motile detergent-extracted cells of *Tetrahymena* and *Chlamydomonas*. *J. Cell Biol.* 96:1610–1621.

Hasegawa, T., S. Takahashi, H. Hayashi, S. Hatano. 1980. Fragmin: a calcium ion sensitive regulatory factor on the formation of actin filaments. *Biochemistry.* 19:2677–2683.

Huang, B. 1986. *Chlamydomonas reinhardtii*, a model system for the genetic analysis of flagellar structure and motility. *Int. Rev. Cytol.* 99:181–215.

Huang, B., A. Mengersen, and V. D. Lee. 1988. Molecular cloning of cDNA for caltractin, a basal body-associated Ca^{2+}-binding protein: homology in its protein sequence with calmodulin and the yeast *cdc 31* gene product. *J. Cell Biol.* 107:133–140.

Huber, M. E., W. G. Wright, and R. A. Lewin. 1986. Divalent cations and flagellar autotomy in *Chlamydomonas reinhardtii* (Volvocales, Chlorophyta). *Phycologia.* 25:408–411.

Keates, R. A. B., and F. R. Hallett. 1988. Dynamic instability of sheared microtubules observed by quasi-elastic light scattering. *Science (Wash. DC).* 241:1642–1645.

Kupfer, A., D. Luovard, and S. J. Singer. 1982. The polarization of the Golgi apparatus and microtubule organizing center in cultured fibroblasts at the edge of an experimental wound. *Proc. Natl. Acad. Sci. USA.* 79:2603–2607.

Lefebvre, P. A., and J. Rosenbaum. 1986. Regulation of the synthesis and assembly of ciliary and flagellar proteins during regeneration. *Annu. Rev. Cell Biol.* 2:517–546.

Lewin, R. A., and C. Burrascano. 1983. Another new kind of *Chlamydomonas* mutant, with impaired flagellar autotomy. *Experientia.* 39:1397–1398.

Lewin, R. A., and K. W. Lee. 1985. Autotomy of algal flagella: electron microscope studies of *Chlamydomonas* (Chlorophyceae) and *Tetraselmis* (Prasinophyceae). *Phycologia.* 24:311–316.

Lewin, R. A., T.-H. Lee, and L.-S. Fang. 1982. Effects of various agents on flagellar activity, flagellar autotomy and cell viability in four species of *Chlamydomonas* (Chlorophyta: Volvocales). *In* Prokaryotic and Eukaryotic Flagella. Society for Experimental Biology Symposium No. 35. W. B. Amos and J. G. Duckett, editors. Cambridge University Press, London. 421–437.

Manton, I. 1964. The possible significance of some details of flagellar bases in plants. *J. R. Microscop. Soc.* 82:279–285.

McDonald, K. 1984. Osmium ferricyanide fixation improves microfilament preservation and membrane visualization in a variety of animal cell types. *J. Ultrastruct. Res.* 86:107–118.

McFadden, G. I., D. Schulze, B. Surek, J. L. Salisbury, and M. Melkonian. 1987. Basal body reorientation mediated by a Ca^{2+}-modulated contractile protein. *J. Cell Biol.* 105:903–912.

Melkonian, M., and H. Robenek. 1980. Eyespot membranes of *Chlamydomonas reinhardtii*: a freeze fracture study. *J. Ultrastruct. Res.* 72:90–102.

Mitchison, T., and M. Kirschner. 1984*a*. Microtubule assembly nucleated by isolated centrosomes. *Nature (Lond.).* 312:232–237.

Mitchison, T., and M. Kirschner. 1984*b*. Dynamic instability of microtubule growth. *Nature (Lond.).* 312:237–242.

Moestrup, Ø. 1982. Flagellar structure in algae: a review, with new observations particularly on the Chrysophyceae, Phaeophyceae (Fucophyceae), Euglenophyceae, and *Reckertia*. *Phycologia.* 21:427–528.

Randall, J., T. Cavalier-Smith, A. McVittie, J. R. Warr, and J. M. Hopkins. 1967. Development and control processes in the basal bodies and flagella of *Chlamydomonas reinhardtii*. *Dev. Biol. Suppl.* 1:43–83.

Ringo, D. L. 1967. Flagellar motion and fine structure of the flagellar apparatus in *Chlamydomonas reinhardtii*. *J. Cell Biol.* 33:543–571.

Rosenbaum, J. L., and K. Carlson. 1969. Cilia regeneration in *Tetrahymena* and its inhibition by colchicine. *J. Cell Biol.* 40:415–425.

Sager, R., and S. Granick. 1954. Nutritional control of sexuality in *Chlamydomonas reinhardtii*. *J. Gen. Physiol.* 37:729–742.

Satir, P. 1976. Cilia, eukaryotic flagella and an introduction to microtubules. *Cold Spring Harbor Conf. Cell Proliferation.* 3:841–846.

Schliwa, M. 1986. The Cytoskeleton an Introductory Survey. Springer-Verlag New York Inc., New York. 326 pp.

Salisbury, J. L., A. Baron, B. Surek, and M. Melkonian. 1984. Striated flagellar roots: isolation and partial characterization of a calcium-modulated contractile organelle. *J. Cell Biol.* 99:962–970.

Salisbury, J. L., A. T. Baron, D. E. Coling, V. E. Martindale, and M. A. Sanders. 1986. Calcium-modulated contractile proteins associated with the eucaryotic centrosome. *Cell Motil. Cytoskel.* 6:193–197.

Salisbury, J. L., M. Sanders, and L. Harpst. 1987. Flagellar root contraction and nuclear movement during flagellar regeneration in *Chlamydomonas reinhardtii*. *J. Cell Biol.* 105:1799–1805.

Salisbury, J. L., A. T. Baron, and M. A. Sanders. 1988. The centrin-based cytoskeleton of *Chlamydomonas reinhardtii*: Distribution in interphase and mitotic cells. *J. Cell Biol.* 107:635–641.

Schulze, D., H. Robenek, G. I. McFadden, and M. Melkonian. 1987. Immunolocalization of a Ca^{2+}-modulated contractile protein in the flagellar apparatus of green algae: the nucleus-basal body connector. *Eur. J. Cell Biol.* 45:51–61.

Stendahl, O. I., and T. P. Stossel. 1980. Actin-binding protein amplifies ac-

tomyosin contraction and gelsolin confers calcium controls in the direction of contraction. *Biochem. Biophys. Res. Commun.* 92:675–681.

Stossel, T. P., C. Chaponnier, R. M. Ezzel, J. H. Hartwig, P. A. Janmey, D. J. Kwiatkowski, S. E. Lind, D. B. Smith, F. S. Southwick, H. L. Yin, and K. S. Zaner. 1985. Nonmuscle actin-binding proteins. *Annu. Rev. Cell Biol.* 1:353–402.

Tamm, S. L. 1988. Iontophoretic localization of Ca-sensitive sites controlling activation of ciliary beating in macrocilia of *Beroë*: the ciliary rete. *Cell Motil. Cytoskel.* 11:126–138.

Tao, W., R. J. Walter, and M. Berns. 1988. Laser-transected microtubules exhibit individuality of regrowth, however most free new ends of the microtubules are stable. *J. Cell Biol.* 107:1025–1035.

Thompson, G. A., C. Baugh, and L. F. Walker. 1974. Nonlethal decilitation of *Tetrahymena* by a local anesthetic and its utility as a tool for studying cilia regeneration. *J. Cell Biol.* 61:253–657.

Tilney, L. G., J. Bryan, D. J. Bush, K. Fujiwara, M. S. Mooseker, D. B. Murphy, and D. H. Snyder. 1973. Microtubules: evidence for 13 protofilaments. *J. Cell Biol.* 59:267–275.

Vigers, G. P. A., M. Coue, and J. R. McIntosh. 1988. Fluorescent microtubules break up under illumination. *J. Cell Biol.* 107:1011–1024.

Watson, M. R., J. M. Hopkins, and J. T. Randall. 1961. Isolated cilia from *Tetrahymena pyriformis*. *Exp. Cell Res.* 23:629–631.

Weiss, R. L., D. A. Goodenough, and U. W. Goodenough. 1977. Membrane particle arrays associated with the based body and with contractile vacuole secretion in *Chlamydomonas*. *J. Cell Biol.* 71:133–143.

Witman, B. B., K. Carlson, J. Berliner, and J. Rosenbaum. 1972. *Chlamydomonas* flagella. I. Isolation and electrophoretic analysis of microtubules, matrix, membranes, and mastigonemes. *J. Cell Biol.* 54:507-539.

Wright, R. L., J. L. Salisbury, and J. Jarvik. 1985. A nucleus-basal body connector in *Chlamydomonas reinhardtii* that may function in basal body localization or segregation. *J. Cell Biol.* 101:1903–1912.